2010 American Control Conference
Marriott Waterfront, Baltimore, MD, USA
June 30-July 02, 2010

A time-varying Kalman filter approach to integral LQG frequency locking of an optical cavity

S. Z. Sayed Hassen and I. R. Petersen

Abstract— **In this paper, we address the problem of frequency locking an optical cavity which arises in the field of quantum optics. The cavity frequency locking problem involves matching the resonant frequency of an optical cavity to that of an incoming laser beam. We model the measurement nonlinearity inherent in the optical cavity and place instantaneous bounds on the observation errors. A convex set within which the error between the laser frequency and the cavity resonant frequency lies is determined and we synthesize a time-varying integral LQG controller which uses information from this set. Simulation results are shown to validate our design in the nonlinear region of operation.**

I. Introduction

A wide range of scientific applications in the field of quantum optics rely on laser frequency stabilization. In particular, laser stabilization forms an integral part of the technology associated with interferometric gravitational-wave detectors; see [1]. The application of lasers in high precision measurement areas is however often restricted by their frequency fluctuations. Thus, different approaches to the frequency stabilization of lasers have been investigated and applied in the physics literature; see, e.g., [2], [3]. A prominent and most widely used method is the Pound-Drever-Hall (PDH) approach; [4], [5]. The error signal generated using this method is proportional to the derivative of the reflected intensity (and is anti-symmetric about resonance) and this signal is used to drive the laser frequency in the appropriate direction. Whilst this scheme works well when the laser frequency is close to the resonant frequency of the cavity (with the error signal being proportional to the reflected intensity of light), it often breaks down when the difference between the two frequencies is large. In particular, the PDH approach becomes unreliable as the derivative of the reflected intensity goes to zero [1]. This problem also occurs in other schemes such as in [6] where the error signal is generated using homodyne detection.

In this paper, we consider an equivalent problem of frequency locking an optical cavity to a laser. We control the length of the optical cavity to adjust its resonant frequency. A piezoelectric actuator is used to regulate the position of one of the cavity mirrors such that the natural frequency of the cavity is locked to the laser frequency. We propose a novel controller design approach which achieves a frequency lock from any given initial operating point. In this way, our approach also caters for large perturbations which can abruptly drive the system away from the linear operating region. This problem has been a difficult one to deal with in the physics community because of an almost complete loss of observability when the system goes out of lock into the nonlinear region.

We propose an approach which works by allowing for unknown but bounded measurement noises in our observations. We determine the set of all frequency errors compatible with the output measurements given the bounded noises. Information from this set is then used to update the parameters of a time-varying Kalman filter at each time instant. In this respect, the filtering problem is related to the deterministic interpretation of the Kalman filter as described in [7] where a set-membership description of the disturbance was used. Our approach also caters for laser phase noise (or $1/f^2$ noise) which acts like a slowly varying disturbance. We introduce integral action into our design through the use of a variant of the integral LQG approach proposed in [8]; see also [6]. A deterministic LQ regulator (see, e.g., [9]) is designed using a suitable cost function and is combined with the state estimates from the Kalman filter to generate the optimal control signal. We conclude by simulating the system under realistic experimental conditions, when it is operating in the nonlinear region.

II. Optical Cavity Locking Problem

We now describe the problem of frequency locking an optical cavity to a laser by varying the length of the optical cavity. Depending on the length of the cavity, the plane waves propagating forward and backward inside the cavity can interact constructively resulting in stable optical modes (resonance) or destructively giving rise to unstable optical modes; see, e.g., [10]. In this way, the piezoelectric actuator regulates the error between the laser frequency and the natural frequency of the cavity. This error is also known as the "detuning variable" and denoted as Δ. The model of the cavity system being considered is made up of two parts:

1) A mechanical subsystem representing the dynamics of the piezoelectric actuator, the controlled mirror and the power amplifier driving the actuator;
2) An optical subsystem representing the dynamics of the optical cavity.

The components in the cavity locking system are depicted in Fig. 1.

The laser mode b of frequency ω_0 is represented by a coherent state $|\beta\rangle$ (represented in Dirac's notation), where β is a real number (without loss of generality), modeled by a boson field $b = b_0 + \beta$. Here b_0 is a vacuum field,

This work was supported by the Australian Research Council

S. Z. Sayed Hassen and I. R. Petersen are with the School of Engineering and Information Technology at the University of New South Wales, Canberra, ACT 2600, Australia. sayed.hassen@gmail.com

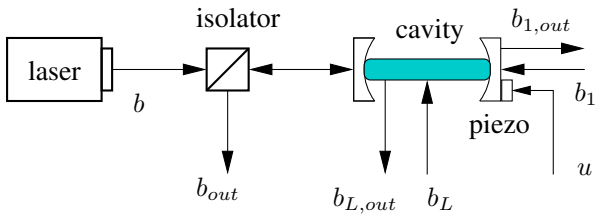

Fig. 1. Cavity locking feedback control loop.

represented as standard quantum Gaussian white noise (with unit variance); see [11]. The cavity is also coupled to two other optical fields: a transmitted mode b_1, and a loss mode b_L. A quadrature of the laser field reflected by the cavity b_{out} is continuously measured using homodyne detection, producing a classical electrical signal y_1. The second measurement we use is y_2, the transmittance obtained from $b_{1,out}$ and represents the transmitted light intensity from the cavity.

III. Modeling

Fig. 2 shows a block diagram of the cavity system under consideration. The control signal u together with a mechanical noise process w feeds into the mechanical subsystem generating Δ at its output. The "detuning" Δ represents the difference between the cavity's resonant frequency from the laser frequency ω_0. However, Δ is not directly available for measurement and instead we have the two measurement signals y_1 and y_2. The signal y_1 is measured using a standard homodyne detection method and includes a sensor noise v_1. Similarly, y_2 is measured using a photodiode and includes a sensor noise v_2. In addition, there are other noise sources that enter the optical cavity which are referred to as quantum noises. These noise sources are discussed in more detail in Sec. III-B.

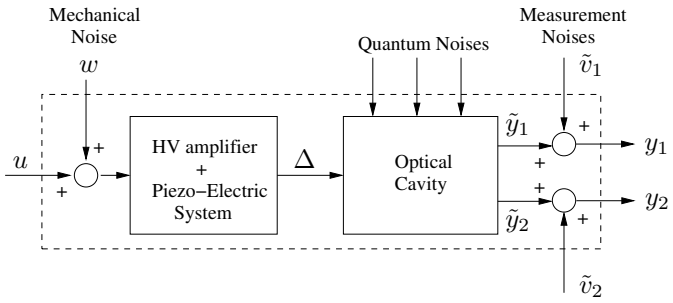

Fig. 2. Block diagram of the cavity system.

A. The Optical Cavity

The cavity is described by the following set of equations (see Fig. 1):

$$\begin{aligned} \dot{a} &= -(\frac{\kappa}{2} - i\Delta)a - \sqrt{\kappa_0}(\beta + b_0) \\ &\quad -\sqrt{\kappa_1}b_1 - \sqrt{\kappa_L}b_L; \\ b_{out} &= \sqrt{\kappa_0}a + \beta + b_0; \qquad (1) \\ b_{1,out} &= \sqrt{\kappa_1}a + b_1. \qquad (2) \end{aligned}$$

Here, a denotes the annihilation operator for the cavity mode, defined in an appropriate rotating frame; see [12], [11]. We have $\kappa = \kappa_0 + \kappa_1 + \kappa_L$, where κ_0, κ_1 and κ_L quantify the strength of the couplings of the corresponding optical fields to the cavity. The measurement signals are determined by the quantities

$$\begin{aligned} \tilde{y}_1 &= e^{-i\phi}b_{out} + e^{i\phi}b_{out}^\dagger \\ &= \sqrt{\kappa_0}(e^{-i\phi}a + e^{i\phi}a^\dagger) + 2\beta\cos\phi + q_0; \qquad (3) \\ \tilde{y}_2 &= b_{1,out}^\dagger b_{1,out} \\ &= \kappa_1 a^\dagger a + \sqrt{\kappa_1}(a^\dagger b_1 + b_1^\dagger a) + b_1^\dagger b_1; \qquad (4) \end{aligned}$$

where $q_0 = e^{-i\phi}b_0 + e^{i\phi}b_0^\dagger$ is a standard Gaussian white noise. The factor $e^{\pm i\phi}$ in (3) arises due to the interaction of the output field b_{out} with the homodyne detector as explained in the next section.

B. Quadrature Measurement

We model the measurement of the X_ϕ quadrature of b_{out} via homodyne detection by changing the coupling operator for the laser mode to $\sqrt{\kappa_0}e^{-i\phi}a$, and measuring the real quadrature of the resulting field. To this end, we re-express the cavity dynamics in terms of the quadrature variables. We write:

$$q = a + a^\dagger; \quad p = i(a^\dagger - a);$$

for the amplitude and phase quadratures respectively. We can now express the cavity dynamics in state-space form as follows:

$$\begin{aligned} \begin{bmatrix} \dot{q} \\ \dot{p} \end{bmatrix} &= \begin{bmatrix} -\frac{\kappa}{2} & -\Delta \\ \Delta & -\frac{\kappa}{2} \end{bmatrix}\begin{bmatrix} q \\ p \end{bmatrix} - \begin{bmatrix} 2\beta\sqrt{\kappa_0} \\ 0 \end{bmatrix} \\ &\quad -\sqrt{\kappa_0}\begin{bmatrix} \cos\phi & \sin\phi \\ -\sin\phi & \cos\phi \end{bmatrix}\begin{bmatrix} q_0 \\ p_0 \end{bmatrix} \\ &\quad -\sqrt{\kappa_1}\begin{bmatrix} 1 & 0 \\ 0 & 1 \end{bmatrix}\begin{bmatrix} q_1 \\ p_1 \end{bmatrix} \\ &\quad -\sqrt{\kappa_L}\begin{bmatrix} 1 & 0 \\ 0 & 1 \end{bmatrix}\begin{bmatrix} q_L \\ p_L \end{bmatrix}; \qquad (5) \\ y_1 &= k_2\sqrt{\kappa_0}\begin{bmatrix} \cos\phi & \sin\phi \end{bmatrix}\begin{bmatrix} q \\ p \end{bmatrix} \\ &\quad + k_2\begin{bmatrix} 1 & 0 \end{bmatrix}\begin{bmatrix} q_0 \\ p_0 \end{bmatrix} + 2k_2\beta\cos\phi + \tilde{v}_1; \qquad (6) \\ y_2 &= \tilde{k}_2\left(\frac{\kappa_1}{4}(p^2+q^2) + \frac{\sqrt{\kappa_1}}{2}\begin{bmatrix} q & p \end{bmatrix}\begin{bmatrix} q_1 \\ p_1 \end{bmatrix}\right) \\ &\quad + \tilde{v}_2; \qquad (7) \end{aligned}$$

with noise quadratures $q_j = b_j + b_j^\dagger$, $p_j = i(p_j^\dagger - q_j)$, for $j = 0, 1, L$ (all standard Gaussian white noises). Here, y_1 is the output of the first sensor in which we have included the noise term $\tilde{v}_1$ and k_2 is the trans-impedance gain of the homodyne detector. Similarly, y_2 represents the measurement of the transmitted light intensity which includes the sensor noise $\tilde{v}_2$ and $\tilde{k}_2$ is the sensor gain of the associated photodiode.

C. Nonlinear Behavior of the Optical Cavity

The system in (5) can be linearized about a given operating point and this would lead to measurement signals which are proportional to the change in frequency of the laser. In turn, this allows for linear control design techniques to be used to control the system, as was done in [6]. The system (5) however behaves linearly only when the variations of Δ about the linearized operating point is small. With the detuning variable Δ treated as an input signal in (5), this system is clearly nonlinear. In this section, we investigate the nonlinear behavior of the measurement signals which will enable us to control the system for large values of Δ. Ignoring the noise terms b_0, b_1 and b_L in (5), we can write

$$\dot{q} = -\frac{\kappa}{2}q - p\Delta - 2\sqrt{\kappa_0}\beta; \quad (8)$$

$$\dot{p} = -\frac{\kappa}{2}p + q\Delta. \quad (9)$$

In most problems of interest, the optical cavity has a very large value of κ and hence a much larger bandwidth compared to that of the mechanical subsystem. Under such conditions, we can safely model the optical cavity as a static nonlinearity which acts on Δ; see Fig. 2. The amplification provided then varies depending on the operating point. To determine the characteristics of this static nonlinearity, we set $\dot{q} = \dot{p} = 0$ in (8) and (9) and obtain

$$\begin{bmatrix} q \\ p \end{bmatrix} = \begin{bmatrix} -\frac{\kappa}{2} & -\Delta \\ \Delta & -\frac{\kappa}{2} \end{bmatrix}^{-1} \begin{bmatrix} 2\sqrt{\kappa_0}\beta \\ 0 \end{bmatrix} = \frac{-1}{(\frac{\kappa}{2})^2 + \Delta^2} \begin{bmatrix} \kappa\beta\sqrt{\kappa_0} \\ 2\beta\sqrt{\kappa_0}\Delta \end{bmatrix}.$$

For the case when $\phi = \frac{\pi}{2}$ in (6), the two measurements available can then be reformulated as:

$$\begin{aligned} y_1 &= k_2\sqrt{\kappa_0}p + 2k_2\beta\cos\phi + v_1 \\ &= -\frac{2k_2\beta\kappa_0\Delta}{(\frac{\kappa}{2})^2 + \Delta^2} + v_1 \quad (\text{since } \cos\phi = 0) \\ &= f_1(\Delta) + v_1; \end{aligned} \quad (10)$$

$$\begin{aligned} y_2 &= k_3(p^2 + q^2) + v_2 \\ &= \frac{k_3\beta^2\kappa_0}{(\frac{\kappa}{2})^2 + \Delta^2} + v_2 \\ &= f_2(\Delta) + v_2. \end{aligned} \quad (11)$$

Here, we have combined all the noise terms together such that:

$$v_1 = \tilde{v}_1 + k_2\, q_0;$$

$$v_2 = \tilde{v}_2 + \frac{1}{2}\tilde{k}_2\sqrt{\kappa_1}\begin{bmatrix} q & p \end{bmatrix}\begin{bmatrix} q_1 \\ p_1 \end{bmatrix};$$

$$\text{and} \quad k_3 = \frac{1}{4}\tilde{k}_2\kappa_1.$$

Using suitable experimental values for the parameters of the optical system (see Table I), the plots shown in Fig. 3 were generated to show the effect of the detuning variable Δ on the measurement signals y_1 and y_2.

It is clear from Fig. 3 that maximum transmission occurs when the detuning variable Δ approaches zero. This occurs when the frequency of the laser's electromagnetic field is equal to the cavity's free spectral range (FSR) = $c/2L$ and repeats itself at integer multiples of the cavity's FSR, where c is the speed of light and L is the controlled length of the cavity.

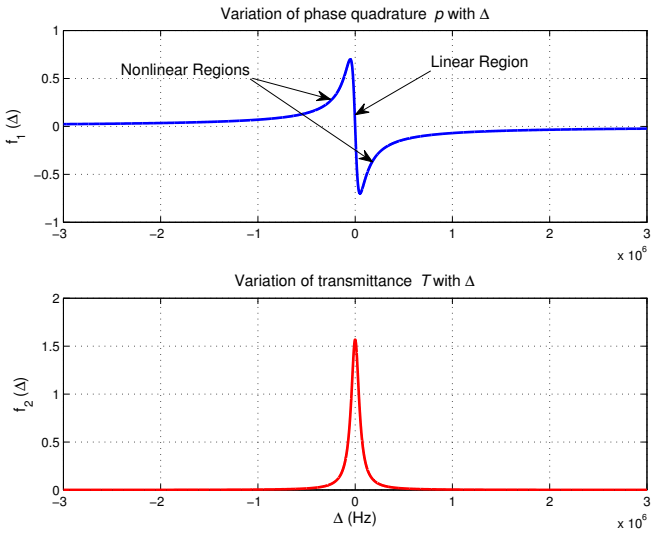

Fig. 3. Behavior of nonlinear measurement functions $f_1(\Delta)$ and $f_2(\Delta)$ with large variations in Δ.

D. Piezoelectric Actuator Model

The piezoelectric actuator model we use for our simulation is the same one obtained experimentally in [6] and which was identified using a subspace identification approach; see [13]. The continuous time linear state-space model is discretized using the ZOH method at a sampling frequency of 50 kHz, resulting in the discrete-time state-space plant model of the form:

$$x_{k+1} = Ax_k + Bu_k;$$

$$\Delta_k = Cx_k. \quad (12)$$

Here, Δ is measured in hertz (Hz) and the control signal u is applied in volts (V).

IV. Main Result

As shown in Fig. 3, the system operates linearly only for small values of Δ. If the system is perturbed strongly enough (which is often the case in practice) and goes outside the linear operating region, it becomes effectively unobservable (with y_1 only as measurement). Outside the linear region, the effective sensor gain may change sign tending to drive the system away from resonance. We seek to construct a control law that would overcome this problem and that would be capable of taking the system from the nonlinear region into the linear region.

Using both measurements y_1 and y_2 to control the cavity system may at first sight seem to provide a trivial solution to the problem. However, both measurement signals tend to zero for large values of $|\Delta|$, as shown in Fig. 3 and in the presence

of measurement noises, the system then becomes extremely sensitive to measurement errors. In the next section, we propose an approach that enables us to estimate the state of a dynamical system using noise corrupted measurements when the measurement noise is assumed to be unknown but bounded.

A. Bounded Noise Model

We consider a model of measurement noise involving instantaneous constraints on the noise variables v_1 and v_2 in (10) and (11) respectively. Thus, we bound the measurement errors v_{1_k} and v_{2_k} at each instant of time k; i.e.,

$$v_{1_k}^2 \leq \mu_1^2; \qquad v_{2_k}^2 \leq \mu_2^2. \tag{13}$$

where μ_1 and μ_2 are fixed constants denoting the magnitude of the noise. Let

$$\begin{aligned} y_{1_k} &= f_1(\Delta_k) + v_{1_k}, \text{ where } f_1(\Delta_k) = \frac{-2k_2\beta\kappa_0\Delta_k}{(\frac{\kappa}{2})^2 + \Delta_k^2}; \\ y_{2_k} &= f_2(\Delta_k) + v_{2_k}, \text{ where } f_2(\Delta_k) = \frac{k_3\beta^2\kappa_0}{(\frac{\kappa}{2})^2 + \Delta_k^2}. \end{aligned}$$

We then consider the problem of characterizing the set of all possible Δ_k compatible with the given observations y_{1_k} and y_{2_k}; i.e., to find the set

$$\begin{aligned} \mathcal{S} = \big\{ &\Delta_k \in \mathbb{R} : (y_{1_k} - f_1(\Delta_k))^2 \leq \mu_1^2 \text{ and} \\ &(y_{2_k} - f_2(\Delta_k))^2 \leq \mu_2^2 \big\}. \end{aligned} \tag{14}$$

It is straightforward to verify that the set $\mathcal{S}$ is equal to the set of $\Delta_k \in \mathbb{R}$ satisfying the inequalities:

$$\begin{aligned} &(16\Delta_k^4 + \kappa^4)(y_{1,k}^2 - \mu_1^2) + 64\Delta_k^3 k_2\beta\kappa_0 y_{1,k} \\ &\quad + 8\Delta_k^2(8k_2^2\beta^2\kappa_0^2 + \kappa^2 y_{1,k}^2 - \kappa^2\mu_1^2) \\ &\quad\quad + 16\Delta_k k_2\beta\kappa_0\kappa^2 y_{1,k} \leq 0; \end{aligned} \tag{15}$$

$$\begin{aligned} &(16\Delta_k^4 + \kappa^4)(y_{2,k}^2 - \mu_2^2) \\ &\quad + 8\Delta_k^2(\kappa^2 y_{2,k}^2 - 4k_3\kappa_0\beta^2 y_{2,k} - \kappa^2\mu_2^2) \\ &\quad\quad - 8\kappa^2 k_3\beta^2\kappa_0 y_{2,k} + 16k_3^2\beta^4\kappa_0^2 \leq 0. \end{aligned} \tag{16}$$

The set $\mathcal{S}$ is constructed by equating the two quartic expressions in (15) and (16) to zero and solving them using Ferrari's equations; see, e.g., [14]. We thus end up with 8 roots $\Delta_{k,i}$ for $i = 1, \cdots, 8$ bounding 9 corresponding regions of interest which are defined as:

$$\begin{aligned} \mathcal{S}_1 &= \{\Delta_k \in \mathbb{R} : -\infty < \Delta_k < \Delta_{k,1}\}; \\ \mathcal{S}_2 &= \{\Delta_k \in \mathbb{R} : \Delta_{k,1} < \Delta_k < \Delta_{k,2}\}; \\ &\vdots \\ \mathcal{S}_8 &= \{\Delta_k \in \mathbb{R} : \Delta_{k,7} < \Delta_k < \Delta_{k,8}\}; \\ \mathcal{S}_9 &= \{\Delta_k \in \mathbb{R} : \Delta_{k,8} < \Delta_k < \infty\}. \end{aligned}$$

The union of the sets $\mathcal{S}_i$, which have a point satisfying (15) and (16), defines the set $\mathcal{S}$. It may be that the set $\mathcal{S}$ is non-convex when the system is operating far from resonance. In those cases, we may end up with two large regions on either side of resonance where the inequalities are satisfied. We then consider the convex hull of the set $\mathcal{S}$.

Given the set conv $\mathcal{S}_k$ at time step k, its center and standard deviation are determined as follows (assuming a uniform probability distribution on conv $\mathcal{S}$):

$$\begin{aligned} \bar{\Delta} &= \frac{1}{2}\left[\min_{\Delta\in\mathcal{S}_k}(\Delta) + \max_{\Delta\in\mathcal{S}_k}(\Delta)\right]; \\ \sigma &= \frac{1}{6}\left[\max_{\Delta\in\mathcal{S}_k}(\Delta) - \min_{\Delta\in\mathcal{S}_k}(\Delta)\right]. \end{aligned}$$

These quantities are used to update the inputs of a discrete-time Kalman filter where they define the new measurement Δ_k and the measurement covariance σ_k^2 respectively. This process is described in the next section.

V. LQG Controller Design

Assuming that the observation errors are bounded, the measurements y_1 and y_2 are used to determine the set $\mathcal{S}$ within which the true value of the detuning variable Δ lies. The center of this set is used as the new measurement $\bar{\Delta}$ and its variance σ^2 is determined from the range of the set $\mathcal{S}$; see Fig. 4.

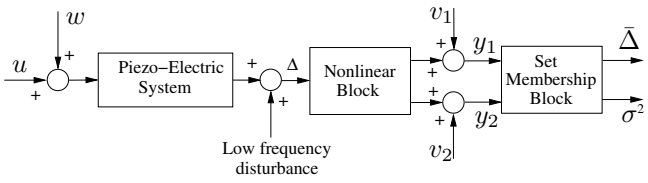

Fig. 4. Complete system model.

The state of a time-varying Kalman filter is updated using the new measurement $\bar{\Delta}_k$ and the variance σ_k^2 available at each instant of time. In this way, the nonlinear problem becomes one which fits into the standard framework of the LQG controller design.

A. LQG cost criterion and Integral action

The LQG controller consists of an estimation block defined by a Kalman filter followed by a deterministic linear quadratic regulator state feedback gain. The regulator assumes that the estimates are the actual states and determines the optimal control law corresponding to a given performance criterion. However the system is also subjected to laser phase noise ($1/f^2$ noise) in the form of low frequency disturbances as well as a large constant disturbance. A standard LQG controller is not able to drive the detuning variable Δ to zero in the face of such disturbances. In order to achieve this, we require integral action and it is included in our LQG design as follows. We use a variant of the integral LQG control scheme initially proposed in [8], where we instead place an integrator at the input of the plant. This modification to the approach of [8] was used to allow for the use of the time-varying Kalman filter as described above. The general setup for the new proposed integral LQG design is as shown in Fig. 5.

We include integral action by introducing an integrator at the output of the controller and split the control signal u into two signals u_1 and u_2 which are generated by the

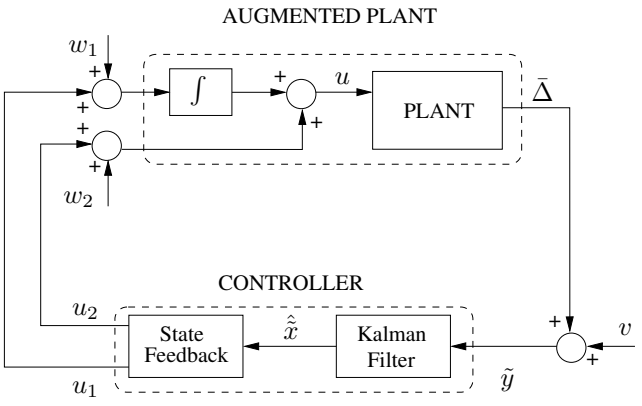

Fig. 5. Integral LQG controller design configuration.

controller. The plant to be controlled as seen by the controller is then the "augmented plant" shown in Fig. 5. When the integral LQG controller is implemented, the integrator is then included as part of the controller. The fictitious process noise w_1 is included to help in the shaping of the controller such that suitable bandwidth and robustness is achieved. The measurement noise v is included to model the variance of the detuning variable $\bar{\Delta}$.

The discretized augmented system we use for the controller design can then be described as follows:

$$\begin{aligned} \tilde{x}_{k+1} &= \tilde{A}\tilde{x}_k + \begin{bmatrix} \tilde{B}_1 & \tilde{B}_2 \end{bmatrix} \begin{bmatrix} u_{1,k} \\ u_{2,k} \end{bmatrix} \\ &\quad + \begin{bmatrix} \tilde{B}_1 & \tilde{B}_2 \end{bmatrix} \begin{bmatrix} w_{1,k} \\ w_{2,k} \end{bmatrix}; \\ \tilde{y} &= \tilde{C}\tilde{x}_k + v_k; \end{aligned} \tag{17}$$

where the mechanical noises $w_{i,k}$ for $i = 1, 2$, are assumed to be Gaussian white noise with variance ϵ_1^2 and ϵ_2^2 respectively. The measurement noise v_k is assumed to be Gaussian white noise with variance σ_k^2. We also assume that the initial state x_0 is unknown but that $x_0 \sim N(\bar{x}_0, P_{x_0})$.

An LQG performance criterion is chosen to minimize the detuning variable Δ while at the same time limit the magnitude of the control signal. This requirement is reflected in the following quadratic cost function:

$$\mathcal{J} = \lim_{k\to\infty} \mathbf{E}\left[\sum_{k=1}^{\infty} (\tilde{x}_k^T Q \tilde{x}_k + u_k^T R u_k)\right]. \tag{18}$$

The matrices Q and R are chosen such that

$$\tilde{x}_k^T Q \tilde{x}_k = |\tilde{y}_k|^2 \text{ and } u_k^T R u_k = r_1|u_{1,k}|^2 + r_2|u_{2,k}|^2 \tag{19}$$

where $r_1, r_2 > 0$ are treated as design parameters. The expectation in (18) is with respect to the Gaussian white noise present in the system. The optimal control is given by

$$u_k = -F\hat{\tilde{x}}_k; \tag{20}$$

where

$$F = (\tilde{B}^T S \tilde{B} + R)^{-1} \tilde{B}^T S \tilde{A}; \tag{21}$$

and S satisfies the algebraic Riccati equation

$$0 = \tilde{A}^T[S - S\tilde{B}(\tilde{B}^T S \tilde{B} + R)^{-1}\tilde{B}S]\tilde{A} - S + Q. \tag{22}$$

B. Discrete-time Kalman Filtering

We now turn our attention to the estimation of the states of the system given a noise corrupted system as described by (17).

If the *a posteriori* estimate and error covariance are given by $\hat{\tilde{x}}_k$ and P_k respectively and $\hat{\tilde{x}}_k^-, P_k^-$ are the respective *a priori* quantities, then the state of the system is estimated recursively using the following Kalman filter equations; see, e.g., [15]:

$$K_k = P_k^- \tilde{C}^T (\tilde{C} P_k^- \tilde{C}^T + \sigma_k)^{-1}, \; P_0^- = P_{\bar{x}_0}; \tag{23}$$

$$\hat{\tilde{x}}_k = \hat{\tilde{x}}_k^- + K_k(\tilde{y}_k - \tilde{C}\hat{\tilde{x}}_k^-), \; \hat{\tilde{x}}_0^- = \bar{\tilde{x}}_0; \tag{24}$$

$$P_k = (I - K_k\tilde{C})P_k^-; \tag{25}$$

and

$$\begin{aligned} \hat{\tilde{x}}_{k+1}^- &= \tilde{A}\hat{\tilde{x}}_k + \tilde{B}u_k; \\ P_{k+1}^- &= \tilde{A}P_k\tilde{A}^T + \tilde{B}W\tilde{B}^T; \end{aligned} \tag{26}$$

where

$$W = \begin{bmatrix} \epsilon_1 & 0 \\ 0 & \epsilon_2 \end{bmatrix}.$$

At each time instant, the new measurement $\tilde{y}_k = \bar{\Delta}_k$ and measurement covariance σ_k are determined from the set $\mathcal{S}$ in (14) and are used to update $\hat{\tilde{x}}_k$ in (24) and P_k using (25) and (23). In designing the LQG controller, the following parameters were chosen for good controller performance. The process noise variances were chosen to be $\epsilon_1^2 = \epsilon_2^2 = 25$ and the control weights were set at $r_1 = 0.01$ and $r_2 = 0.1$.

VI. Simulation Results

We simulate the system with the given control law (20) for a time period of 10 ms and with a sampling rate of 50 kHz. The simulation parameters used reflect those of an experimental setup used in our optics laboratory and the noise models are specifically chosen to reflect experimental conditions. The parameters and the selected bounds on the noise inputs are shown in Table I.

Simulation parameters	Value	Units
β	7×10^7	Hz
κ	1×10^5	Hz
κ_0	1×10^4	Hz
k_2	5×10^{-8}	V/Hz
k_3	8×10^{-9}	V
μ_1	1×10^{-2}	V
μ_2	1×10^{-2}	V

TABLE I
Simulation Parameter Values

The system is initialized outside the linear region, with $\Delta = -1 \times 10^6$ Hz. Moreover, we include a disturbance on Δ to represent the low-frequency laser phase noise. This disturbance is modeled as integrated white noise with an initial offset of -1×10^6 Hz as shown in Fig. 6.

The process noise w_2 is modeled as Gaussian white noise with variance $\sigma_1^2 = 1 \times 10^{-4}$ and w_1 being a fictitious process

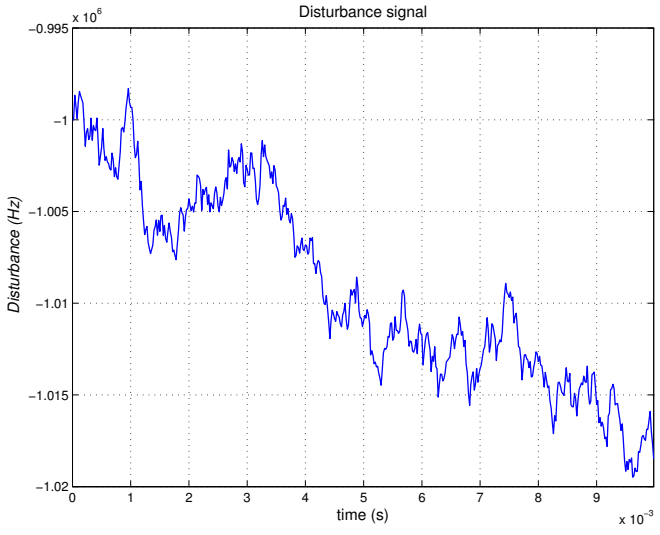

Fig. 6. Laser phase noise modeled as integrated white noise with an initial offset of -1 MHz.

noise input (used for the controller design process only) is ignored in the simulation stage. The measurement noises v_1 and v_2 are uniformly distributed and bounded such that

$$v_1^2 \leq \mu_1^2; \qquad v_2^2 \leq \mu_2^2.$$

Fig. 7 shows the variation of the two measurement signals y_1 and y_2 representative of the phase quadrature p (V) and the transmittance I (V) respectively. The measurement signal y_1 is highly sensitive to small disturbances. The transmittance I reaches and settles close to its peak value after about 4 ms.

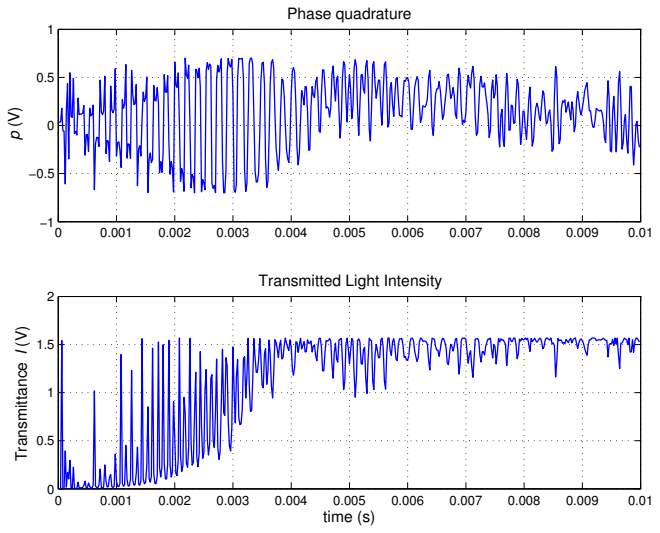

Fig. 7. Phase quadrature and transmittance measurement.

The controller is effective in transferring the system from the nonlinear region into the linear region and regulates Δ close to zero in the presence of process noise, laser phase noise as well as bounded measurement noises on the two measurement channels y_1 and y_2. The oscillatory response seen is due to the resonant nature of the specific piezoelectric actuator, as modeled in [6].

VII. Conclusion

In this paper, we have addressed the problem of stabilizing a nonlinear optical cavity system which arises in experimental quantum optics. Taking advantage of the different time-scales in the interconnected systems, the piezoelectric actuator together with the inherent nonlinearity present in the optical cavity were modeled separately. Instantaneous error bounds were placed on the two measurement noises and the set of all frequency errors Δ consistent with the given output measurements is determined. Information from the set $\mathcal{S}$ is used to update the estimate of the states and the nonlinear problem is treated as an integral LQG control problem with a time-varying Kalman filter. Simulation results show that the controller is successful in regulating the detuning variable Δ in the presence of realistic noise models. Future research will involve validating our design on an experimental laboratory system.

Acknowledgment

The authors wish to thank Assoc. Prof. E. H. Huntington for numerous research discussions.

References

[1] E. D. Black, "An introduction to Pound-Drever-Hall laser frequency stabilization," *Am. J. Phys.*, vol. 69, no. 1, pp. 79–87, 2001.
[2] A. D. White, "Frequency stabilization of gas lasers," *IEEE J. Quantum Elec.*, vol. 1, no. 8, pp. 349–357, 1965.
[3] T. W. Hansch and B. Couillaud, "Laser Frequency Stabilization by Polarization Spectroscopy of a Reflecting Reference Cavity," *Optics Communications*, vol. 35, no. 3, pp. 441–444, Dec. 1980.
[4] R. V. Pound, "Electronic frequency stabilization of microwave oscillators," *Review of Scientific Instruments*, vol. 17, no. 11, pp. 490–505, 1946.
[5] R. W. P. Drever, J. L. Hall, F. V. Kowalski, J. Hough, G. M. Ford, A. J. Munley, and H. Ward, "Laser Phase and Frequency Stabilization using an Optical Resonator," *Applied Physics B*, vol. 31, pp. 97–105, 1983.
[6] S. Z. Sayed Hassen, M. Heurs, E. H. Huntington, I. R. Petersen, and M. R. James, "Frequency locking of an optical cavity using linear-quadratic Gaussian integral control," *J. Phys. B: At. Mol. Opt. Phys.*, vol. 42, no. 17, p. 175501, Sept. 2009.
[7] D. P. Bertsekas and I. B. Rhodes, "Recursive State Estimation for a Set-Membership Description of Uncertainty," *IEEE Trans. Autom. Control*, vol. 16, no. 2, pp. 117–128, Apr. 1971.
[8] M. J. Grimble, "Design of optimal stochastic regulating systems including integral action," *Proc. IEE Control & Science*, vol. 126, no. 9, pp. 841–848, Sept. 1979.
[9] H. Kwakernaak and R. Sivan, *Linear Optimal Control Systems*. John Wiley & Sons, Inc., 1972.
[10] A. E. Siegman, *Lasers*. University Science Books, 1986.
[11] C. W. Gardiner and P. Zoller, *Quantum noise*. Springer, Berlin, 2000.
[12] H. A. Bachor and T. C. Ralph, *A guide to experiments in quantum optics*. John Wiley, 2004.
[13] T. McKelvey, H. Akçay, and L. Ljung, "Subspace-based multivariable system identification from frequency response data," *IEEE Trans. Autom. Control*, vol. 41, no. 7, pp. 960–979, 1996.
[14] D. M. Burton, *The history of mathematics: An introduction*. Allyn and Bacon, Boston, 1985.
[15] R. G. Brown, *Introduction to random signal analysis and Kalman filtering*. John Wiley & Sons Ltd., 1983.